INERTIAL CONFINEMENT FUSION (ICF)

More generally laser produced plasmas: producing X-rays (lithography, contact microscopy), hydrodynamic experiments, ICF, calibration

Contents

Principles of ICF

For fusion conditions to be reached by inertial confinement a small solid pellet of D-T must be compressed to a density of 10^3 to 10^4 times that of the pellet particle density $n_s = 4.5 \times 10^{22}$ cm^{-3}. Proposal are to irradiate the pellet symmetrically. A plasma is produced on the pellet surface. This plasma expands, exciting spherical shock waves that propagate inward, compressing the remaining pellet.

Let the pellet gain η_G be the output of the nuclear fusion energy E_f to the input laser (or a particle beam) energy E_I delivered to the pellet. The heating efficiency is denoted by η_h. Let n, T be the density and volume. Assume $T_e = T_i = T$, and we have

$$E_f = \frac{n^2}{4}\langle\sigma v\rangle Q_{DT}\alpha V\tau$$

$$3nTV = \eta_h E_I$$

α is an enhancement factor due to alpha particle heating. The volume $V = 4\pi r_c^3/3$ with r_c the compressed pellet radius, and τ is the confinement time

$$\tau = \frac{r_c}{v_T}$$

Here v_T is the thermal velocity. Q_{DT} = 17.6 MeV is the sum of alpha and neutron energies (Q_n = 14.1 MeV, Q_α = 3.5 MeV). Then we can write

$$E_f = nV\alpha\frac{Q_{DT}}{2}\frac{n}{2}\langle\sigma v\rangle\tau = nV\alpha\frac{Q_{DT}}{2}\eta_b$$

$$\eta_b = \frac{n}{2}\langle\sigma v\rangle\tau$$

Since $Q_{DT}/2$ is the fusion energy output per ion, η_b is the fuel burn ratio. The ratio

$$\eta_T = \frac{Q_{DT}/2}{3T}\alpha$$

is the thermonuclear gain, because one ion and one electron are together of energy 3T. Then we can combine these efficiencies to get

$$\eta_G = \eta_h\eta_b\eta_T$$

and

$$\tau = \frac{2\eta_b}{n\langle\sigma v\rangle} = 0.3x10^{-6}\eta_b\left(\frac{n_s}{n}\right)$$

$$r_c = v_T\tau = \frac{2\eta_b v_T}{n\langle\sigma v\rangle} = 0.2\eta_b\left(\frac{n_s}{n}\right)$$

$$E_I = \frac{1}{\eta_h}3nT\frac{4\pi}{3}\left(\frac{2\eta_b v_T}{n\langle\sigma v\rangle}\right)^3 = 8x10^{12}\frac{\eta_b^3}{\eta_h}\left(\frac{n_s}{n}\right)^2$$

where we have taken T = 10 keV, and expressed the plasma density in terms of the solid density $n_s = 4.5x10^{28}$ m^{-3}, used $v_T = 7x10^5$ ms^{-1} and $\langle\sigma v\rangle = 1.5x10^{-22}$ ms^{-1}. The thermonuclear gain $\eta_T = 293\alpha$. Assume the fuel burn ratio $\eta_b = 0.3$, and the heating efficiency $\eta_T = 0.1$, then the pellet gain $\eta_G = 8.8\alpha$, and for $n/n_s = 10^4$ we have

$E_I = 22$ kJ, $\tau = 9$ ps, and $r_c = 6.3$ μm

Note we are restricted to a conversion efficiency $\eta_E < 0.4$ from E_F to electrical energy.

When the compressed density is very high the mfp of the alpha particle is of order r_c, so that alpha heating can occur. If the alpha energy is distributed evenly, then one alpha can heat about 100 ions to thermonuclear burn temperatures of 10 keV, because $3.5x10^6/3/(10x10^3) \approx 100$ ions. Therefore the upper limit on the enhancement factor α is about 100 x 14.1 MeV/17.6 MeV ≈ 80.

The condition $\eta_E\eta_I\eta_G > 2$ is necessary to make usable electricity. For lasers η_i, the conversion efficiency of electrical energy to laser energy, is only about 0.05, so that the pellet gain $\eta_G > 2/(0.4x0.05)$, i.e. $\eta_G > 100$ (e.g. $\eta_h = 0.1$, $\eta_b = 0.3$, $\eta_T = 3300$, implying $\alpha = 11$).

Targets - simple picture

Targets are micro shells of polymer, overcoated with plasma polymer to provide a thick ablator layer which absorbs the laser energy and drives the compression. Targets must compress symmetrically. Raleigh Taylor instabilities that arise during implosion can lead to a mixing of shell and fuel.

Recent experiments use hohlraums with 1 to 5 atmospheres of gas, which might be H/He mixtures, or hydrocarbons. Windows are placed over the laser entrance holes to contain the gas.. A low mass window is used to minimize use of laser energy during its burn. Windows have been made of silicon nitride, thickness 0.25 μm. These break, so polymides are being tested.

The gold targets are made by electroplating or electroforming gold onto a sacrificial copper mandrel, which is then removed using nitric acid. A small hole is drilled for gas passage. Hypodermic tubing is epoxy bonded over the hole. The widows are also epoxy bonded over the holes. Targets must withstand 15 psi (normal fill pressure). Diagnostic openings have 7 mm titanium epoxied over them. D gas plastic shells may be inside which have a half life of 30 hours.

A direct drive target is typically a glass spherical container coated with metal or polymeric fill and filled with a DT mixture, and some diagnostic gas. Direct drive targets can be filled with the D-T mix by diffusion at a high temperature and pressures up to 200 atm.

Inverted corona targets are spherical shells with holes for laser radiation. The inside surface of the shell is covered with a heavy hydrogen compound. e.g. BeD_2 can be deposited by evaporation of metallic Be deuteride.

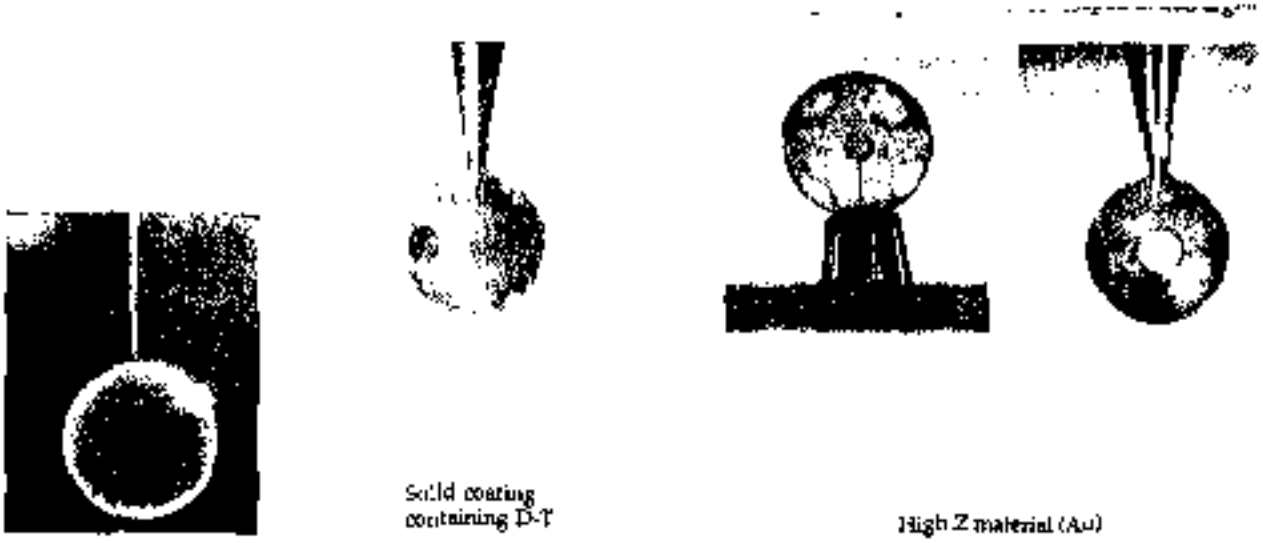

Targets for laser "Iskra-4," "Iskra-5" system: (a) — radiograph of a direct drive target (
glass shell coated with polyparaxylene); (b) — inverted corona target with the containing D-T
film (BeD_2, BeDT, TiD_x, TiD_xT_{y-x}, $(CD2)_n$, or $(CD_xT_{2-x})_n$); (c) — indirect drive target.

Facilities available

OMEGA

(University of Rochester) A 60 beam glass laser for direct drive. Will require 1 mm diameter targets.

NIKE

(NRL) A KrFl laser for direct drive.

NIF

(LLNL) A glass laser with 1.8 MJ at third harmonic. The hohlraum is heated to about 300 eV. The radius of the central ignition hot spot is intended to be 1/36 of the original pellet radius. The hohlraum design has $r_W/r_p = 2.5$ at the equator. Targets will be about 2 mm diameter.

The fuel can be a solid or liquid D-T layer about 100 μm on the inside surface of the pellet.

NOVA

(LLNL) The convergence is currently 25, plastic shell thickness 30 μm, pulse width 1 ns. D2 filled multiple layer shells used, about 0.5 mm diameter. Experiments on Nova use laser produced plasmas to generate X-rays capable of back lighting dense, cold plasmas (density = 1 to 3 gm cm-3, T = 5 to 10 eV, areal density ρ = 0.01 to 0.05 g/cm^2). X-rays used vary from 80 eV to 9 keV. Allows probing of plasmas relevant to hydrodynamic experiments. Typical diagnostics are 100 ps pinhole framing camera and time integrated CCD camera for short pulse back lighter.

TRIDENT

(LANL) A frequency doubled Nd glass driver (527 nm), 2 beams of up to 250 J each, for pulses of typically 80 to 2,000 ps. (50 J for a 100 ps pulse, 250 J for a 1 to 2 ns pulse). The minimum spot size is < 100 μm.

Indirect drive: a Hohlraum cavity

Cylindrical gold can with entrance holes at each end, a pair of laser beam rings, and a spherical pellet in the center. Laser light heats walls to T_{r1}. The X-ray emmission and the sideways thermal conductivity then heat the remainder of the cavity wall to a somewhat lower temperature T_{r2}. The local X-ray emmission is then $I \quad T_r^4$. The radiation is assumed to have an axis of symmetry, so that Legendre Polynomials can be used

$$I_{wall} = \sum_{n=0}^{\infty} A_n P_n(\cos(\theta))$$

and the smaller pellet absorbs the radiation with an intensity

$$I_{pellet} = \sum_{n=0}^{\infty} \varepsilon_n A_n P_n(\cos(\theta))$$

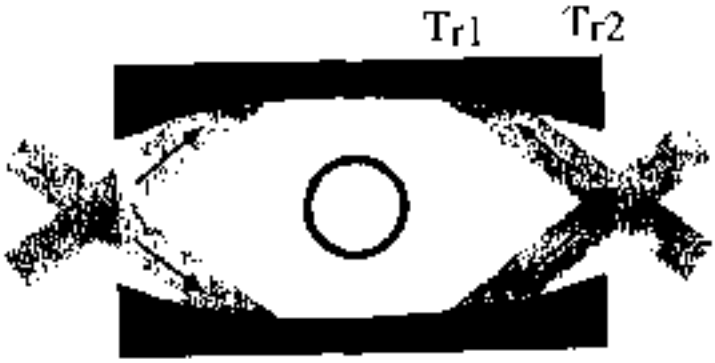

The original hohlraum concept used one pair of laser beams, with a can-shaped gold wall. The wall is heated locally to temperature T_{r1}, and the x radiation then heats the rest of the wall to an average temperature $T_{r2} < T_{r1}$.

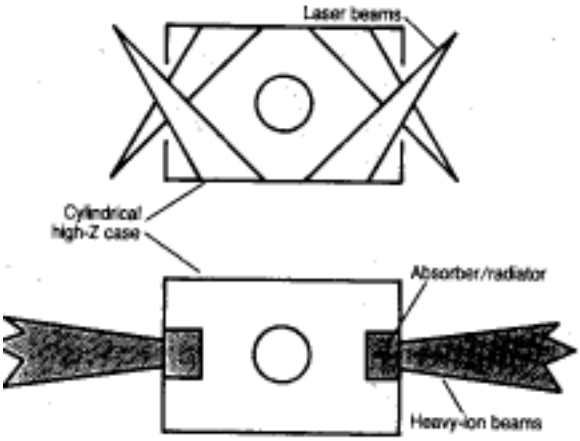

Calculations showed that the plasma blowoff from a gold wall filled the hohlraum to a density high enough to collisionally absorb most of the laser light near the entrance hole. The laser deposition then leads to a pole high asymmetry. Even if the light could reach the hohlraum wall, another possible asymmetry exists. At the beginning of the implosion the wall is only locally heated, and T_{r2} in the first figure is nearly zero. Later T_{r2} approaches T_{r1}, and the wall heating introduces its own equator high asymmetry (because of the entrance holes). The figure below shows how Lindl proposed to solve these problems. To reduce asymmetries produced by the gold ablation the hohlraum is filled with a gas mixture of helium and hydrogen (about 1 mg/cc). The laser light has less collisional absorption in the low Z gas and can propagate to the walls. To control the residual time dependent asymmetry resulting from the secondary heating of the walls, the laser light is distributed into inner and outer rings, and the power distribution is varied between these two rings.

Typical pulses for NIF will have a 12 - 16 ns foot, followed by a high power pulse of about 4 ns. The foot duration is determined by the time it takes lower temperature X-rays to drive an initial shock through the pellet shell, establishing a smooth pressure gradient in the shell. Otherwise , if the shell is preheated by a strong shock, high compression is prohibited,

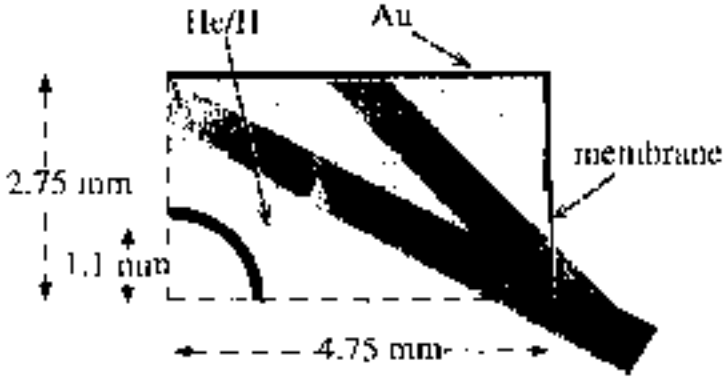

Geometry of NIF target. Two laser rings; gold wall; ~ 1 mg/cc of He/H gas fill; membrane to hold in gas fill; central pellet

The last figure shows the results of a calculation of what might actually happen. Parameters to be calculated include the fraction of laser power converted to X-rays, and the fraction converted into heating the gold plasma that fills the hohlraum. How well does the gas hold back the plasma? Present code results predict for the NIF a 70% conversion of laser light energy to X-rays with a temperature of about 300 eV. There are worries that introducing the low Z fill to the hohlraum will introduce laser filamentation and stimulated Brillouin scatter, both of which will destroy symmetry.

As the NIF hohlraum evolves in time, the wall moves inward with a complicated structure. With more wall motion where the laser energy is directly deposited. Some of the energy in the inner laser ring may be absorbed and refracted by the CH blowoff from the pellet. The membrane that held in the gas fill could also modify the laser target interaction.

Targets and their manufacture

Micro encapsulation.

A problem is the elimination of vacuoles, micron sized voids in the thin shell wall, probably originating from the formation of small, water rich regions during the evacuation of organic solvents from the shell. When the micro-encapsulated droplet is first formed, the liquid shell consisting of organic solvents and dissolved polymer is devoid of water. Agitation of the water bath in which the drop is suspended ensures that the organic solvent is constantly swept away by unsaturated water. This convective mass transfer provides a strong force for solvent removal. Shell hardening occurs as the polymer concentration increases. Water has a small but non zero solubility in the organic phase so that before much of the solvent has left, water diffuses rapidly into the shell. Therefore as the solvent level drops, water is trapped in the shell and becomes supersaturated. Phase separation into water rich regions can occur by homogeneous nucleation, or heterogeneous condensation. use 770C, initial radius 0.75 mm, wall thickness 0.25 mm, initial wall of 37% toluene, 53% 1,2-dichloroethane, 10% polystyrene. (all by weight)

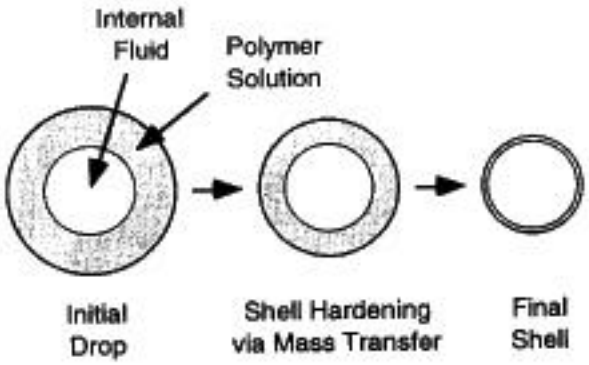
Internal
Fluid
Polymer
Solution
Initial
Drop
Shell Hardening
via Mass Transfer
Final
Shell

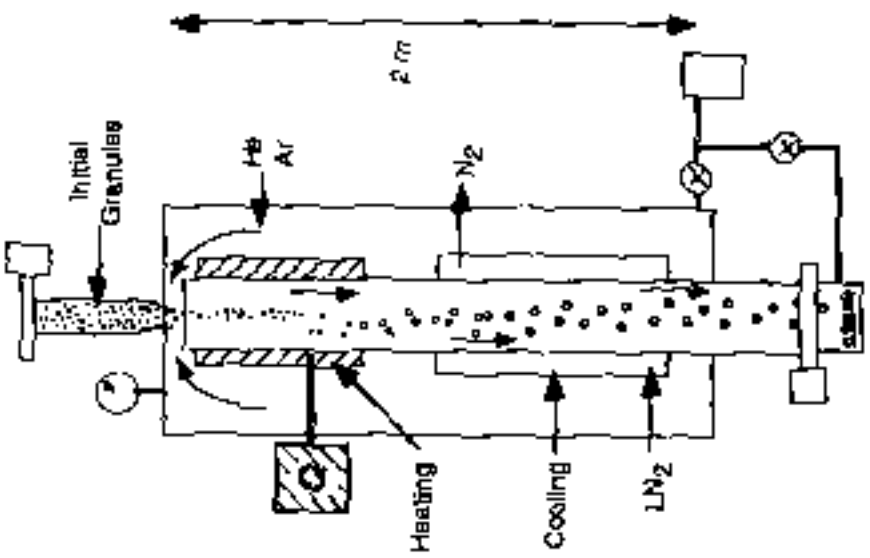

Figure 1. Shown is the general scheme of the droptower furnace. Note upper heating and lower cooling systems. Details shown are not to scale.

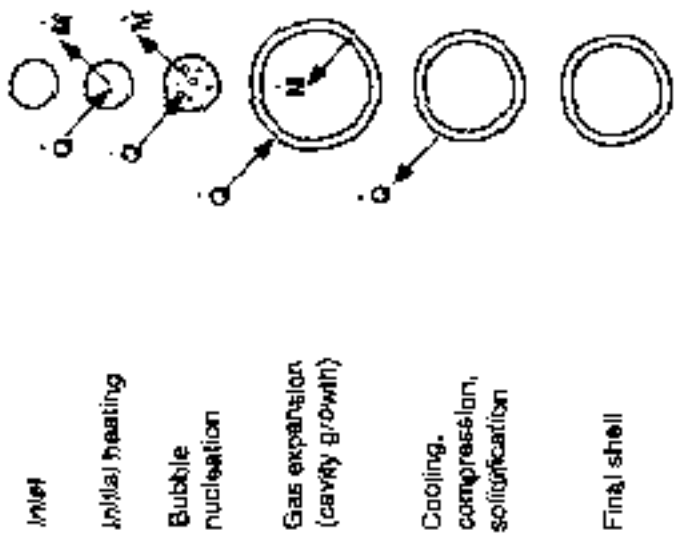

Figure 2. The process of shell formation in the hot zone involves both heat and mass transfer, as well as gas bubble nucleation events.

Drop tower techniques

Start with solid polystyrene pellets with a distribution of masses in the range a few hundred micrograms. These are produced by suspension polymerization. Size of pellets determined by mixer design and stabilization agents, typically polyvinyl alcohol and a copolymer of methacrylic acid and methylmethacrylate. Next infuse a foamer - either during the initial suspension or subsequently by diffusion e.g. toluene, heptane, about 5% by weight.

The droptower is a 3:1 helium argon gas at about 5 kPa (10^5 Pa = 1 atmosphere). Granules released at top, heated as they fall. Temperature is about 1000 ^{0}C. Granules foam at 130 ^{0}C. At 500 to 700 ^{0}C high quality shells are formed, with radius about 1 to 1.5 mm.

Non contact coating methods.

Use a gas dynamic levitation with lower nozzle and upper collector.

Depolymerizable mandrels

Want to produce capsules with custom internal walls. Use depolymerization of polyalpha methylstyrene (PAMS) mandrels. An irregular commercial pellet of desired mass is softened in hot water to allow surface tension to produce a spherical pellet. The bead is then overcoated with plasma polymer. This is then placed in an oven at 300 ^{0}C, where the PAMS depolymerizes to gas and diffuses out leaving a hollow shell.

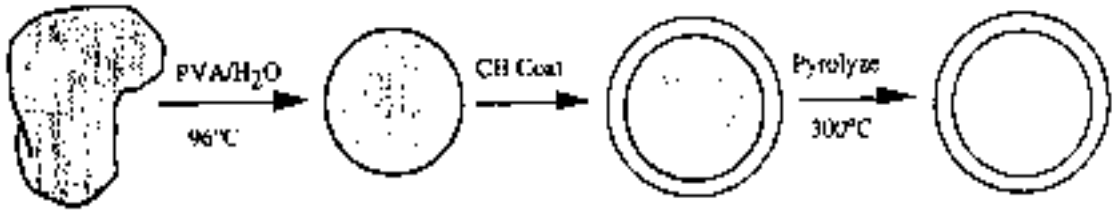

Hollow shells can be produced by starting with a poly(α-methylstyrene) bead, then overcoating with thermally more stable plasma polymer. The coated bead is pyrolyzed at 300 °C for 30 hours or more leaving a spherical hollow shell.

The plasma coating system consists of a supply manifold with controlled gas flow, an RF discharge generator, a coating chamber and a vacuum pump. The polymer deposition occurs in a glow discharge. The reactive fragments produced in the discharge chemically combine on nearby surfaces to form a coating.

Foam shells

The fuel can be a solid or liquid DT layer about 100 μm on the inside surface. One way to do this is to use a spherical target with a inner low density foam layer to help support and symmetrize the fuel layer. Transparent foam shells are needed to allow for optical characterization. The opacity is usually due to the scattering of light from a large (>1 μm) cell structure. The basic approach is to make resorcinol/formaldehyde shells by micro encapsulation. The method involves producing a water droplet encapsulated by an oil layer with about 4% weight trimethacrylate monomer, which is in turn suspended in an aqueous bath. For R/F systems the phases are reversed, because the polymerizable reactants are water rather than oil soluble. Thus an oil in water in oil system is needed.

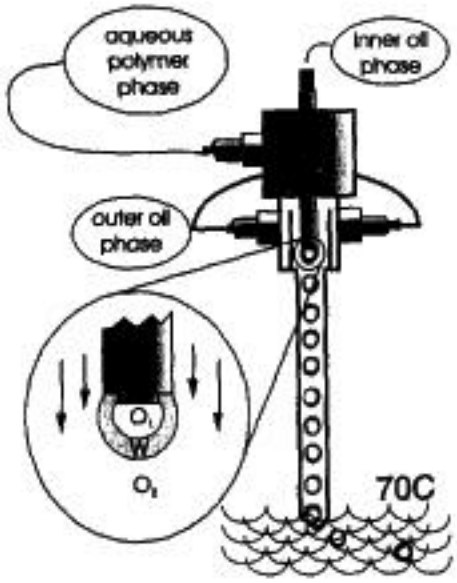

The R/F preforms consist of a droplet of an oil phase, O_1, encapsulated by the aqueous R/F formulation, indicated by W. These droplets are stripped from the two inner orifices by a second organic phase, O_2 which flows into a stirred, heated solution of density matched O_2.

Spinning targets

why: improve stability to Raleigh Taylor modes by rotational shear flow

how: ablation force with a non zero azimuthal component (e.g. by structuring the pellet layers with a fully axisymmetric radial irradiation), or a left-right asymmetric structure within the pellet.

Velocity must increase as implosion occurs: would get factor C = 25 increase on NOVA. Need final rotational velocity of order implosion velocity, i.e. ≈ 3×10^7 cm/s, so initial v ≈ 10^6 cm/s. Final rotational energy is C^2 times the initial one, so initial rotational energy is C^2 times less (i.e. 2×10^{-3} of the total mechanical energy).

Azimuthal torque must be transferred to deeper layers - but viscosity too low. Therefore use longer-time, low E pulse before main pulse to start spinning.

Magnetic field generation

Generalized Ohm's law, neglecting electron inertia and ion pressure

$$\bar{E} + \bar{v} \times \bar{B} = \eta \bar{J} + \frac{1}{en}\left(\bar{J} \times \bar{B} - \quad p_e\right)$$

The jxB term is called the Hall term, and together with the last term is often neglected. But keeping the last term, we will find a field generation. We know that a circuit moving through a magnetic field with a velocity v produces a magnetic flux over a surface S spanning the circuit

$$\frac{d\varphi}{dt} = \frac{\partial}{\partial t}\int_S \bar{B} \cdot d\bar{S} - \oint\left(\bar{v} \times \bar{B}\right) \cdot \, d\bar{l}$$

$$= \oint\left(\frac{p_e}{ne} - \eta \bar{J}\right) \cdot \, d\bar{l}$$

Therefore the term $p_e/(ne)$ generates a magnetic field as long as $n \times T \neq 0$. A thermoelectric term in the Ohms law will also lead to a magnetic field generation.

DIAGNOSTICS

Diagnostics:

Optical -	time integrated:	35 mm SLR (film)
		spectrometers (film, 200 - 1100 nm)
	time resolved:	photodiodes (200 to 1100 nm, 60 or 270 ps),
		streak camera (400 - 1100 nm, 30 ps/mm)

	gated:	holographic interferometer (4 frames, 100 ps)
X-ray	time integrated	pinhole cameras (film)
		grating spectrometers (transmission, 0.2 - 2 keV)
		crystal spectrometers (film and CCD, 3 to 35 keV)
	time resolved	streak camera (film: > 5 eV, 15 ps/mm; XRD: > 5 eV, 150 ps,)
	gated	gated X-ray imager (film, 0.5 to 5 keV, 80 ps, 16 frame)

Spectra

Absolutely calibrated crystal spectrometers and X-ray diodes used to measure properties of the back lighters. Generated with incident laser radiation of $10x10^{14}$ Wcm^{-2} of 0.53 μm (green) light for 1 to 2 ns onto solid planar targets. Use uranium, aluminum, molybdenum, scandium, titanium, iron.

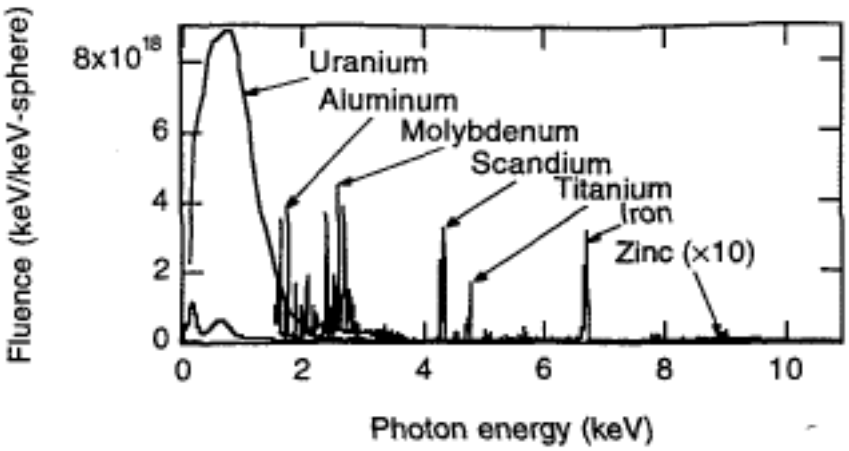

Need to smooth the laser beam. Use random phase plate rpp. Phase errors across the beam diameter result in large uncontrolled intensity variations. However laser beam can be divided into a large number of overlapping beamlets whose diffraction size is matched to a target. This overlap eliminates large scale spatial non uniformities at the expense of small scale interference (speckles) between the beamlets. One approach to smoothing is to introduce an RPP at the output. This has a large number of elements each of which has a phase shift of 0 or π relative to adjacent elements. The pattern of phase shifts is distributed in a quasi random manner over the surface of the plate. In addition temporal incoherence is added, then the small scale pattern moves around, resulting in a time asymptotic pattern of uniform intensity.

Figure 2. X-ray images of laser produced plasmas from uranium used for x-ray backlighting. The image on the left was produced by a beam without a random phase plate (RPP); structure in the laser beam reproduces in the x-ray spot. The image on the right used a RPP.

Large area back lighters.

Typically use Sc, Ti, Fe, filtered with the same element at the diagnostic to select the He-α line. A monochromatic spectrum is best, but a single line is not necessary. e.g. back lit implosion. Study Rayleigh Taylor (RT) instability, and its effects on fuel temperature, convergence, neutron yield, use dopants in ablated pusher to maintain high areal density. (dopant prevents energetic x-rays in the drive from depositing in the pusher). The pusher areal density is an important parameter. It is determined by the attenuation of the back lighter x-ray flux and compared with simulations. Witness ball: replace real target with low density ball, in which asymmetry effects are more noted. (exaggerates shock asymmetries)

Typical set up

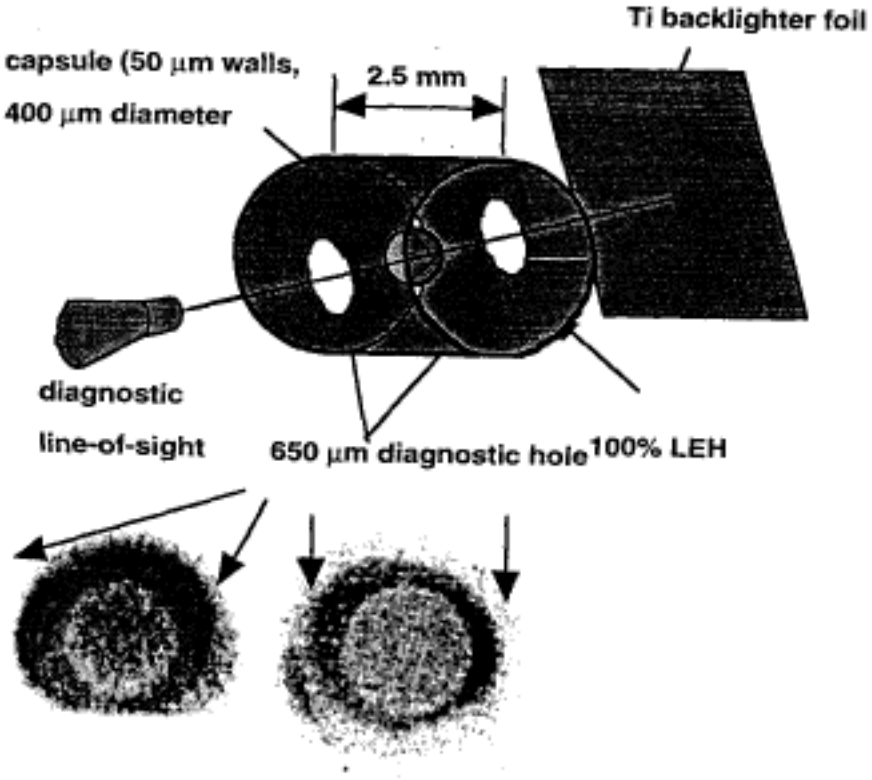

Figure 3. Experimental setup and typical images from backlit implosion and witness ball experiments. The pusher may be seen as a lighter ring (lower transmission) in the left hand image; in the image on the right a lighter ring is also visible but in this case it is due to the shock compression of the solid witness ball material. The 4.7 keV Ti He-α backlighter is essentially unattenuated by the ablated material surrounding the capsule.

Rayleigh Taylor experiments

Observable is modulation in transmission of a large area back lighter which corresponds to modulations in optical depth of a foil. As the opacity of the foil is constant to keV x-rays, the modulation represents areal density modulations. The modulation arises from sinusoidal ripples present on the surface. The foil is accelerated by the ablation and the ablation surface is RT unstable. The modulations are expected to grow exponentially, become nonlinear, and saturate. Foil can be direct or indirect drive accelerated. Use prefilter (12 μm Be) to stop X-rays below 1 keV.

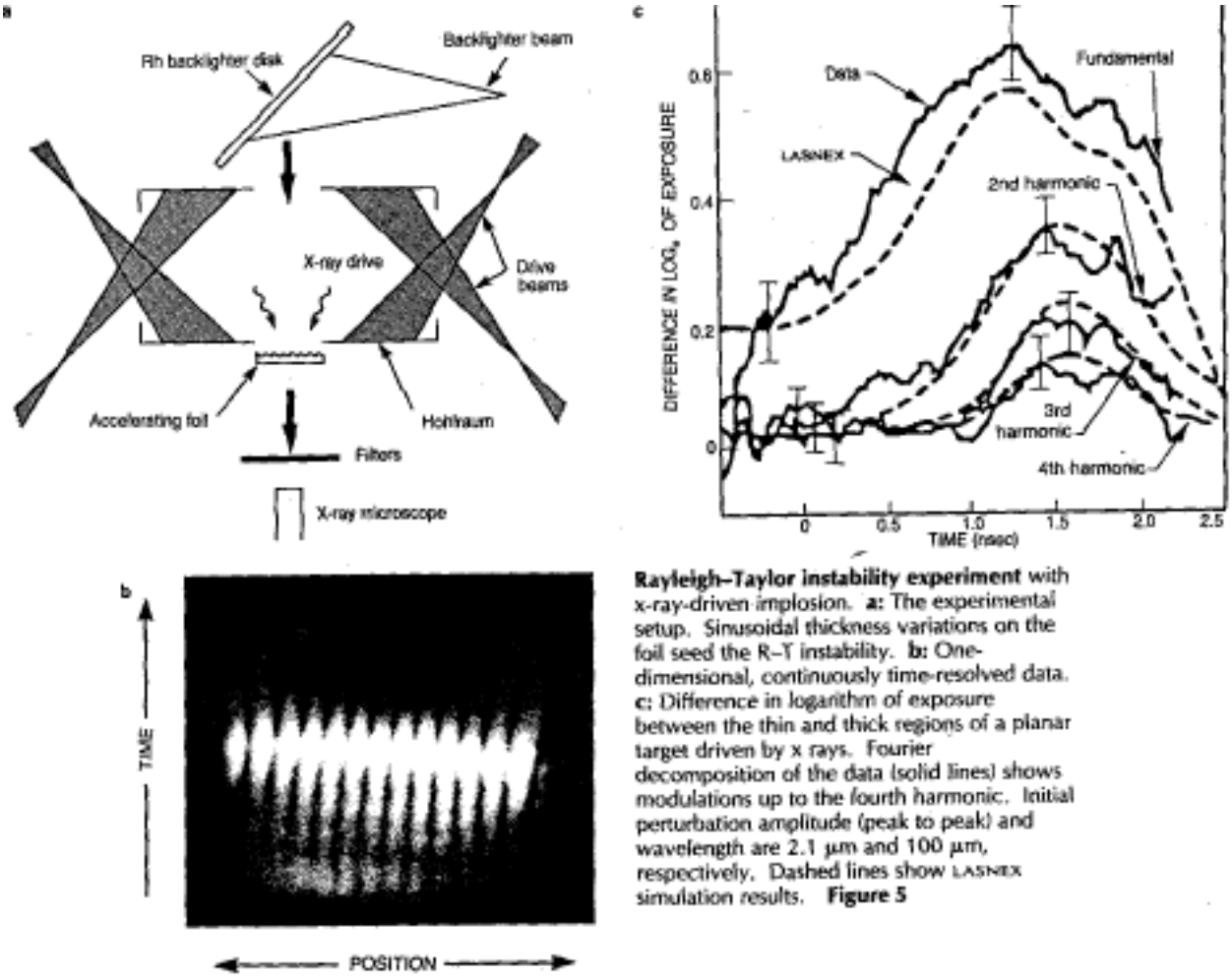

Rayleigh–Taylor instability experiment with x-ray-driven implosion. **a:** The experimental setup. Sinusoidal thickness variations on the foil seed the R–T instability. **b:** One-dimensional, continuously time-resolved data. **c:** Difference in logarithm of exposure between the thin and thick regions of a planar target driven by x rays. Fourier decomposition of the data (solid lines) shows modulations up to the fourth harmonic. Initial perturbation amplitude (peak to peak) and wavelength are 2.1 μm and 100 μm, respectively. Dashed lines show LASNEX simulation results. **Figure 5**

Another example, showing modulation at the 30 μm fundamental. Structures running perpendicular to imposed perturbations are due to laser drive. Back lighter illuminates lower part of foil in first frame, progressing downward until last frame it illuminates upper part. This is an effect of parallax as the images are formed by lower and lower pinholes in the array. Hence back lighter must be large enough to overfill the area that must be illuminated when gated mcp cameras are the diagnostic.

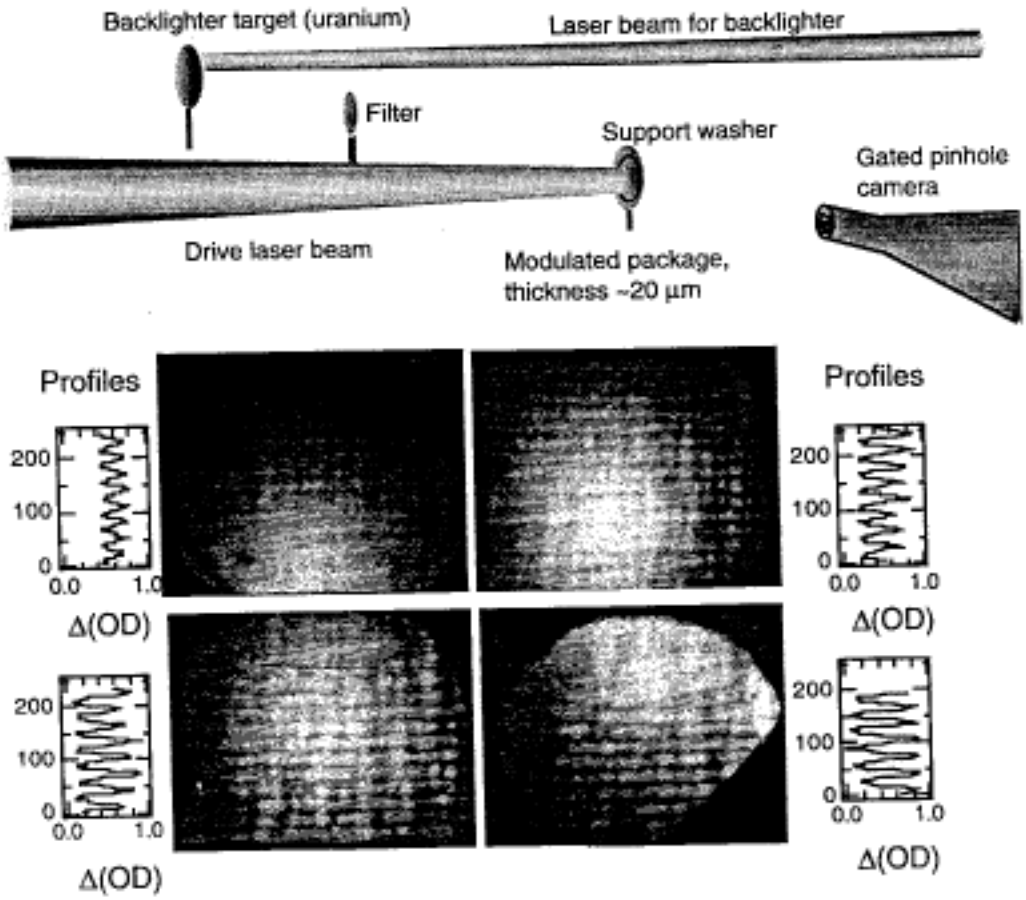

Figure 6. Experimental setup for direct-drive planar Rayleigh-Taylor experiments. The images are (left right and top to bottom) at t=1.0, 1.5, 2.0, and 2.5 ns after the start of the drive laser pulse. The size of ea image is 700 μm. The initial wavelength was 30 μm and the initial amplitude 0.25 μm.

Point back lighters

Use a laser produced plasma which is very small. The spatial extent of the point back lighter determines the spatial resolution. Advantages: high laser light intensity at focus means 10^{16} Wcm^{-2} and then 10 keV x-rays. uniform illumination, resolution with a fiber as the target is comparable to pinhole camera. But source size increases with time.

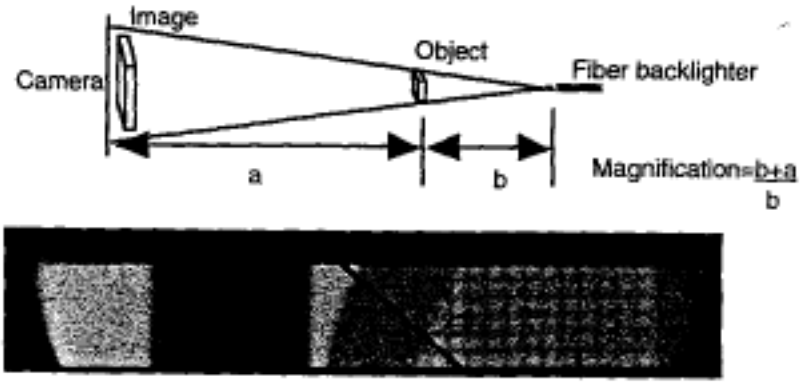

Figure 11. Point backlighter geometry and image of a resolution grid. The backlighter was a round Zn fiber 1⁴ μm in diameter, the pulse duration was 100 ps and the magnification was 18.

Rayleigh Taylor instability

Equilibrium

$$p = \boldsymbol{j} \times \boldsymbol{B} - \rho \quad \varphi$$

use Maxwell with E constant in time so that $\times \boldsymbol{B} = \mu_0 \boldsymbol{j}$:

$$p = \boldsymbol{j} \times \boldsymbol{B} - \rho \quad \varphi = \frac{\boldsymbol{B} \cdot \quad \boldsymbol{B}}{\mu_0} - \quad \frac{B^2}{2\mu_0} - \rho \quad \varphi$$

$\boldsymbol{B} \cdot \quad \boldsymbol{B}$ tension term from curvature disappears for straight systems. the B^2 term represents stresses due to mutual repulsion of lines of force. equivalent to pressure.

Potential energy of plasma is

$$W = \int \left(\frac{B^2}{2\mu_0} + \frac{3}{2} p + \rho\varphi \right) dV$$

volume V includes any vacuum region, φ is gravitational potential. Without any dissipation the total energy is conserved (i.e. sum of W and any kinetic energy).

Let an equilibrium system be perturbed by a displacement x, a function of the initial position. To first order in x the change $\partial W = 0$, since this is the definition of an equilibrium. The stability is determined by the sign of $\partial W(x,x)$, the value of ∂W keeping terms of order x^2. If $\partial W(x,x)$ is positive the KE cannot exceed the initial value ∂W and the perturbation cannot grow.

If $\partial W(x,x)$ is negative, $|\partial W|$ and the KE can grow together as x2 increases, and we are unstable. More quantitatively

$$\frac{1}{2}\int \rho\left(\frac{dx}{dt}\right)^2 dV + \partial W(x,x) = 0$$

now let x exp(-iωt)

$$\omega^2 = \frac{\partial W(x,x)}{\frac{1}{2}\int \rho x^2 dV}$$

Thus if ∂W is negative, ω is imaginary, and the perturbation grows.

Changes to potential energy ∂W from three terms, ∂W_S at the interface, ∂W_p from deformations within the plasma, and ∂W_v, the change in magnetic energy in any vacuum regions.

Consider ∂W_S at an interface between plasma and vacuum. The plasma pressure changes discontinuously across the surface S, parallel to the lines of force.. Let x_n be the perturbation normal to the surface. The force F per unit area across the interface which is proportional to x_n. The total work done on the fluid in the course of moving x_n is

$$\delta W_S = -\frac{1}{2}\int \boldsymbol{x}_n \cdot \boldsymbol{F}(x_n) dS$$

In equilibrium the total pressure across the interface is

$$p + \frac{B^2}{2\mu_0}$$

As x_n increases, the pressure on the two sides of S changes in different ways, since $_n\left(p + B^2/(2\mu_0)\right)$ is different n the two sides. $F(x_n)$ is the product of x_n times this increase in gradient as the surface is crossed in the direction of increasing x_n:

$$\delta W_S = \frac{1}{2}\int x_n^2 \left\langle {}_n\left(p + \frac{B^2}{2\mu_0}\right)\right\rangle dS$$

where <...> means the change in some quantity.

When the direction of B is everywhere the same, an instability arises if the plasma is supported by a magnetic field against the gravitational force $\rho\mathbf{g}$ per cm^3, or if the magnetic field

is accelerating the plasma against the equivalent reaction force, -ρd**v**/dt. For the case of sharp interfaces, with different densities and field strengths, we can obtain the growth rate. The equilibrium equation is (see first equation, keep gravitational terms, no currents)

$$\frac{d}{dx}\left(p + \frac{B^2}{2\mu_0}\right) = -\rho g$$

The gravitational force is included: the acceleration g is directed in increasing x. Now the equation for the change in energy across the surface becomes

$$\delta W_S = -\frac{1}{2}\langle\rho\rangle g \int x_n^2 \, dS$$

This is negative if density of upper layer exceeds that of lower layer. If positive x is taken in direction of **g**, then - sign in above two equations go to plus, but definition of <ρ> means this also changes sign, so we are left again with δW_S negative.

Choose x constant along lines of force, then no change in magnetic energy - they move as rigid rods.

Must consider change in potential energy resulting from deformations within the plasma. These will be negligible as long as wavelength is small compared to scale height ρ/gradρ. Therefore δW is negative if a dense plasma is supported by a lighter plasma against gravity, provided direction of B is uniform. Same is true if a lighter plasma accelerates a denser plasma by pushing it.

Unstable perturbation leads to flutes parallel to the lines of force. suppose

$$x_x = Ae^{\pm kx}\sin(ky)$$
$$x_y = \pm Ae^{\pm kx}\cos(ky)$$
$$x_z = 0$$

with minus above interface, plus below. Then

$$\omega^2 = -gk\frac{\langle\rho\rangle}{2\bar{\rho}}$$

where $\langle\rho\rangle$ is jump in ρ, $\bar{\rho}$ is average across the surface.

Femto-second laser produced plasmas

High intensity short pulse lasers produce ultra short x-ray pulses. 1981: 1 ns $C0_2$ laser at kJ level showed that potential at focus produced superhot electrons which when incident on solid target produced bremsstrahlung In 1992 Kmetec reported similar results with 125 fs 40 m, 5 Hz pulse. Laser pulse absorption and x-ray conversion efficiency are determined by wavelength of laser, irradience, polarization, angle of incidence. These govern the temporal behavior and spatial gradients of plasma electron temperature and density and gradients. Solid targets absorb laser power over a skin depth (100A, and in heated region Te about 100 to 1000 eV. Thermal X-rays about 1 keV and above are produced. . Strong gradient and high density means that rapid quenching of x-rays occur by thermal conduction into underlying cold material and hydrodynamic expansion. Besides collisional absorption, resonance and non- collisional absorption matter. These nonlinear processes give bremsstrahlung radiation and Kα from target.

Supernova simulation

RT is important in larger scale experiments - supernovae. These have strong density gradients and can be RT unstable. In the nonlinear regime (amplitude > wavelength) the amplitude grows at terminal bubble velocity

$$u = 0.36\sqrt{g\lambda}$$

g is acceleration of interface, λ is wavelength. Suggests a characteristic time scale

$$\tau = \frac{\lambda}{u} \approx \sqrt{\frac{\lambda}{g}}$$

Now transform from supernova to lab, so that

$$\lambda_{sn} = a_1 \lambda_{lab}$$
$$g_{sn} = a_2 g_{lab}$$

then

$$\tau_{sn} = \sqrt{\frac{a_1}{a_2}} \tau_{lab}$$

e.g. a type II 25 M_{sun} supernova, then spatial scale is 10^{10} cm, acceleration is 10^{3} cm-2, time scale is 10^{4} s. For lab experiment scale is 10^{-4} cm, so $a_1 = 10^{14}$. The acceleration is 10^{14} cm-2, so $a_2 = 10^{-11}$. Therefore the time scale in the lab should be $10^{4}/(10^{25})^{1/2}$, i.e. about 1 ns. Other parameters which would not sale (density, temperature, mode number, perturbation amplitude/wavelength, are very similar.

So you might mimic a supernova with a laser driven implosion. Need strong density gradients: use copper foil pushing a plastic layer.